Spherical Rectification Based Stereo Vision Applied to Hybrid Dual Camera Vision Systems

Stefano Cagnoni[1], Monica Mordonini[1], Luca Mussi[2], and Giovanni Adorni[3]

[1] Università degli Studi di Parma, Dipartimento di Ingegneria dell'Informazione
{cagnoni,monica}@ce.unipr.it
[2] Università degli Studi di Perugia, Dipartimento di Matematica e Informatica
mussi@dipmat.unipg.it
[3] Università degli Studi di Genova, Dipartimento di Informatica Sistemistica e Telematica
adorni@unige.it

Abstract. Spherical reprojection was introduced in omnidirectional vision mainly to simplify the projection model for single-viewpoint catadioptric sensors. It was then extended to omni-stereo systems to perform 3D information recovery and disparity map estimation. Although the same rectification technique has already been exploited also to the classical stereo-vision problem, no one has described its natural application to Hybrid Dual Camera Systems yet. This is what we are going to highlight in this paper by presenting all the geometrical relationships characterizing such systems. A critical assessment of some practical results is also reported in the last section.

1 Introduction

In the last decade some investigations on hybrid dual camera systems have been made [1–7]. The joint use of a standard moving camera and of a catadioptric sensor provides these sensors with different and complementary features: while the traditional camera can be used to acquire detailed information about a limited region of interest (as in human "foveal vision"), the omnidirectional sensor provides wide-range, but less detailed, information about the surroundings (as in human "peripheral vision"). This class of vision systems can be applied to tasks such as video surveillance and mobile robot navigation. Their particular configuration makes it possible to define several different strategies to control the orientation of the standard camera; for example, scattered focus on different objects permits to perform recognition/classification tasks while continuous movements allow for tracking moving objects. Three-dimensional reconstruction based on stereo vision is also possible, although less directly than when standard stereo configurations are used.

Stereo vision algorithms need to find homologous projections of a certain point on a stereo image pair in order to be able to estimate its position in the 3D space. To simplify this search problem, reducing it to a mono-dimensional search, most known algorithms rely on homography-based epipolar rectification

Workshop Proceedings of SIMPAR 2008
Intl. Conf. on SIMULATION, MODELING and PROGRAMMING for AUTONOMOUS ROBOTS
Venice(Italy) 2008 November,3-4
ISBN 978-88-95872-01-8
pp. 366-376

techniques (referred to as *planar rectification*) which ensure that an image pair is obtained, which has corresponding (straight) epipolar lines at the same y (or x) coordinate in both images. Unfortunately, planar rectification has many limitations and, especially when the two cameras are heavily misaligned, rectification may produce unbounded or badly deformed images. Obviously, this is not a problem when dealing with standard stereo rigs which ensure a good camera alignment; unfortunately, this is not the case when dealing with hybrid dual camera systems, essentially because of the different nature of the two cameras and because of their relative positioning. Not least, the rectification of images characterized by very large fields of view on planar surfaces could result in the introduction of major detail deformation, making the use of classical feature matching techniques impossible.

Although the concept of spherical rectification for depth estimation is not new, recent work have tried to highlight its suitability for omnidirectional cameras, or camera equipped with fisheye lenses, [8, 9], as well as for dual PTZ cameras systems [10]. Reported results are promising, also for the possible generation of depth/disparity maps based on the images obtained with this rectification. Even more interest about this technique could arise once equiresolution catadioptric sensor (see for example [11, 12]), which intrinsically capture spherical images, will be more spread and popular.

In this paper, we would like to show how the spherical image rectification procedure can be easily applied also to hybrid dual camera vision systems. In the next two sections, supposing that the reader is confident with classical stereo, epipolar and catadioptric geometry, we present all the details needed to understand this technique, while in sections 4 we present some results we obtained using both synthetic and real images.

2 Geometrical Framework

Without loss of generality we suppose that the catadioptric sensor be placed above the other camera without any constraint in their relative positioning (see figure 1).
Let $\boldsymbol{O}_o$ be the single viewpoint of the omnidirectional camera and $\boldsymbol{O}_t$ be the viewpoint of the traditional camera. Suppose that, at any time, we are able to derive, from the calibration data, the coordinates of $\boldsymbol{O}_o$ and $\boldsymbol{O}_t$ with respect to the global reference frame w that is centered in $\boldsymbol{O}_w$, as well as the orientation matrices ${}^w_o\mathrm{R} = [{}^w\boldsymbol{x}_o\, {}^w\boldsymbol{y}_o\, {}^w\boldsymbol{z}_o]$ and ${}^w_t\mathrm{R} = [{}^w\boldsymbol{x}_t\, {}^w\boldsymbol{y}_t\, {}^w\boldsymbol{z}_t]$. Under these conditions, the baseline L of the stereo-system can be easily computed as the length of the segment $\overline{\boldsymbol{O}_o\boldsymbol{O}_t}$, i.e. $L = |\overline{\boldsymbol{O}_o\boldsymbol{O}_t}|$. Furthermore, we define a reference frame s centered in $\boldsymbol{O}_s \equiv \boldsymbol{O}_t$ to be used for spherical rectification: its orientation can be expressed by ${}^w_s\mathrm{R} = [{}^w\boldsymbol{x}_s\, {}^w\boldsymbol{y}_s\, {}^w\boldsymbol{z}_s]$ where:

$$ {}^w\boldsymbol{z}_s = \frac{{}^w\boldsymbol{O}_o - {}^w\boldsymbol{O}_t}{L}, \quad {}^w\boldsymbol{y}_s = {}^w\boldsymbol{z}_s \times {}^w\boldsymbol{z}_t, \quad {}^w\boldsymbol{x}_s = {}^w\boldsymbol{y}_s \times {}^w\boldsymbol{z}_s \tag{1} $$

This way, $\boldsymbol{z}_s$ is parallel to the baseline and the azimuth of $\boldsymbol{z}_t$ with respect to the frame s is zero.

Workshop Proceedings of SIMPAR 2008
Intl. Conf. on SIMULATION, MODELING and PROGRAMMING for AUTONOMOUS ROBOTS
Venice(Italy) 2008 November,3-4
ISBN 978-88-95872-01-8
pp. 366-376

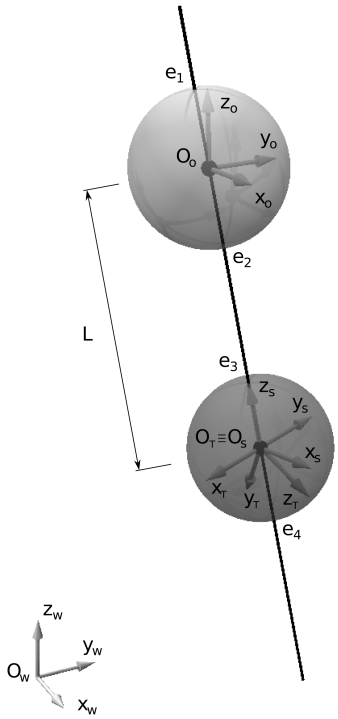

Fig. 1. Geometrical framework for the spherical rectification of the images acquired by the dual camera system.

Imagining the two sensors to be spherical cameras with the *image planes* defined by the *unit spheres* centered in $\boldsymbol{O}_o$ and $\boldsymbol{O}_t$ and aligned with frame s, we have the four *epipoles* at $e_{1,2} = (\boldsymbol{O}_o \pm \boldsymbol{z}_s)$ and $e_{3,4} = (\boldsymbol{O}_t \pm \boldsymbol{z}_s)$. Considering a point $\boldsymbol{P}$) in the free space, the *epipolar plane* $\Pi(\boldsymbol{O}_o, \boldsymbol{O}_t, \boldsymbol{P})$ intersects the unit spheres at vertical great circles with constant zenithal angle. Moreover, the segment $\overline{\boldsymbol{O}_o\boldsymbol{P}}$ intersects the upper sphere at (ϕ_o, θ_o), while $\overline{\boldsymbol{O}_t\boldsymbol{P}}$ intersects the lower sphere at (ϕ_t, θ_t) (coordinates being in the form $(zenith, azimuth)$).

Considering the half of the epipolar plane $\Pi(\boldsymbol{O}_o, \boldsymbol{O}_t, \boldsymbol{P})$ characterized by azimuth $\theta_o = \theta_t$, we have the situation depicted in figure 2: the point $\boldsymbol{P}$ and the two viewpoints form a scalene triangle of which we can measure one side (the baseline L) and the two angles α and β. In fact, the coordinates of $\boldsymbol{P}$ in the two spherical images are directly related with the zenithal angles ϕ_o and ϕ_t and with the azimuthal angles θ_t and θ_o (not visible in figure 2) as aforesaid.

Hence, once ϕ_o, ϕ_t and θ_t (or θ_o) are meaasured, we can estimate the side a of the triangle and write the point P in spherical coordinates referred to the system's frame s as:

Workshop Proceedings of SIMPAR 2008
Intl. Conf. on SIMULATION, MODELING and PROGRAMMING for AUTONOMOUS ROBOTS
Venice(Italy) 2008 November,3-4
ISBN 978-88-95872-01-8
pp. 366-376

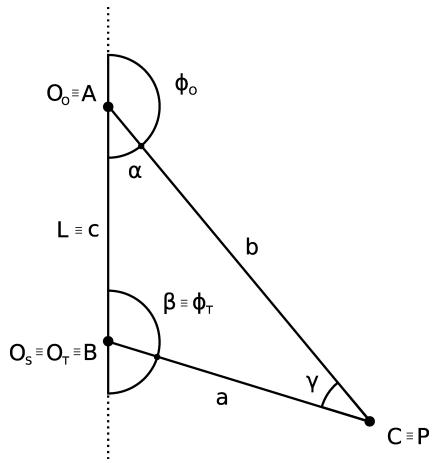

Fig. 2. Geometrical relationships on a generic epipolar plane $\Pi(\boldsymbol{O}_o, \boldsymbol{O}_t, \boldsymbol{P})$: the ASA theorem can be applied to the scalene triangle $\overset{\triangle}{ABC}$ to solve for side a (or b).

$$r_s = \frac{L\ \sin\phi_o}{\sin(\phi_o - \phi_t)}, \quad \theta_s = \theta_t = \theta_o, \quad \phi_s = \phi_t \tag{2}$$

which becomes the following (after a brief reorganization) in Cartesian coordinates:

$$x_s = \frac{L\ \cos\theta_t}{\cot\phi_t - \cot\phi_o}, \quad y_s = \frac{L\ \sin\theta_t}{\cot\phi_t - \cot\phi_o}, \quad z_s = \frac{L\ \cot\phi_t}{\cot\phi_t - \cot\phi_o} \tag{3}$$

It could be noticed that the common term $\frac{L}{\cot\phi_t - \cot\phi_o}$ in equation 3 corresponds to the distance between the point P and the baseline L.

Therefore, ${}^s\boldsymbol{P}$ can be expressed in the global reference frame by applying the roto-translation which describes the stereo system:

$${}^w\boldsymbol{P} = {}^w\mathrm{R}_s\,{}^s\boldsymbol{P} + {}^w\boldsymbol{O}_s \tag{4}$$

3 Spherical Rectification

To proceed with the spherical rectification of the two images, we have to define an equiangular sampling grid on the unit sphere, taking the frame s as reference for the spherical coordinate system. To completely specify this grid, all we need is the number of samples (cells) along with the azimuthal and zenithal directions: let them be n_θ and n_ϕ, respectively. We obtain a $n_\theta \times n_\phi$ grid with a θ-step of $2\pi/n_\theta$ and a ϕ-step of π/n_ϕ: to obtain "squared" cells it is thus necessary to set $n_\theta = 2n_\phi$. The spherical coordinates of the sample at row i and column

Workshop Proceedings of SIMPAR 2008
Intl. Conf. on SIMULATION, MODELING and PROGRAMMING for AUTONOMOUS ROBOTS
Venice(Italy) 2008 November,3-4
ISBN 978-88-95872-01-8
pp. 366-376

j are then $\big(\theta\text{-step}(i+0.5), \phi\text{-step}(j+0.5)\big)$. This sampling grid can finally be unwrapped on a planar surface to get a regular grid with squared "pixels": these pixels must be filled with appropriate color values to be taken from the images acquired by the sensor.

To this aim we have to consider two different sampling grids, RI_o and RI_t, superimposed on the unit spheres centered in the two single-viewpoints. Furthermore, it is necessary to have two projection functions able to relate the coordinates of a point $\boldsymbol{P}$ in the space, or merely its projections on the unit spheres, with the coordinates of its homologous representations in the omnidirectional image, OI, and the traditional image, OT, acquired by the stereo-sensor. Let them be $f_o : \mathbb{R}^3 \rightarrow \mathcal{P}_o$ and $f_t : \mathbb{R}^3 \rightarrow \mathcal{P}_t$, with $\mathcal{P}_o$ and $\mathcal{P}_t$ being the set of all pixel belonging to OI and OT respectively. In the end, the two grids can be filled by means of the following relations:

$$\begin{array}{l} I\big(RI_o(i,j)\big) = I\big(f_o(\boldsymbol{P}_{o_{i,j}})\big), \quad \forall i,j \in \mathbb{N}, \quad 0 \leq i < n_\phi, \quad 0 \leq j < n_\theta \\ I\big(RI_t(i,j)\big) = I\big(f_t(\boldsymbol{P}_{t_{i,j}})\big), \quad \forall i,j \in \mathbb{N}, \quad 0 \leq i < n_\phi, \quad 0 \leq j < n_\theta \end{array} \tag{5}$$

being

$$\begin{array}{l} \boldsymbol{P}_{o_{i,j}} = \boldsymbol{O}_o + cartesian\big(1.0, \theta\text{-step}(i+0.5), \phi\text{-step}(j+0.5)\big) \\ \boldsymbol{P}_{t_{i,j}} = \boldsymbol{O}_t + cartesian\big(1.0, \theta\text{-step}(i+0.5), \phi\text{-step}(j+0.5)\big) \end{array} \tag{6}$$

and $cartesian(r, \theta, \phi) : \mathbb{R}^3 \rightarrow \mathbb{R}^3$ the classical function that converts spherical coordinates into Cartesian ones. Obviously, knowing the optical aperture of the traditional camera, $\boldsymbol{z}_t$ and consequently narrowing the range of i and j, it is possible to generate rectified images limited to the common field of view of the two cameras, hence saving a lot of computation time.

This procedure could clearly produce the loss of information or the introduction of a certain noise depending on the resolution chosen for the rectified images: the number of cells on the grids should hence be carefully chosen. Furthermore, a more sophisticated procedure than the one reported in equation 5, which exploits also some interpolation techniques, should be employed.

It is worth noticing that there are no restrictions for f_o and f_t since they can be either exact closed-form projection function or some polynomial approximation. In particular, f_o could be the mapping function proposed in [13] or could be like the ones proposed, for example, in [14, 4].

4 Experimental Results

To assess the effectiveness of spherical rectification applied to Dual Camera Sensors, we performed several tests involving both image reprojections, to verify the correct correspondence among epipolar lines, as well as 3D point coordinate reconstruction, to assess the evaluation error. This should be mostly due to the noise introduced by image quantization and to non-exact data obtained from the calibration procedures.

Workshop Proceedings of SIMPAR 2008
Intl. Conf. on SIMULATION, MODELING and PROGRAMMING for AUTONOMOUS ROBOTS
Venice(Italy) 2008 November,3-4
ISBN 978-88-95872-01-8
pp. 366-376

4.1 Synthetic Images

Prior to switch to real-world images, we wanted to work in a synthetic environment, to ensure a reasonable confidence about geometrical data such as camera placement and orientation, lens distortion, object positions and dimensions, etc. To do so, we simulated a 3D environment using POV-Ray[4].

Figure 3 shows the two images, obtained by a simulated dual camera system through which it is possible to observe a very simple virtual room: the one on the left derives from a hyper-catadioptric camera that was placed above a traditional camera which points slightly below the horizon line and captures the right image. It is worth noticing that no particular constrictions were taken into account in setting the relative placement of the two cameras. Without listing all geometrical characteristics of the system, which would be of no interest here, we only show the rectified image pair for the whole sphere and for the common field of view in figure 4: as can be seen from the detail, epipolar lines are perfectly aligned and oriented along the vertical axis as expected.

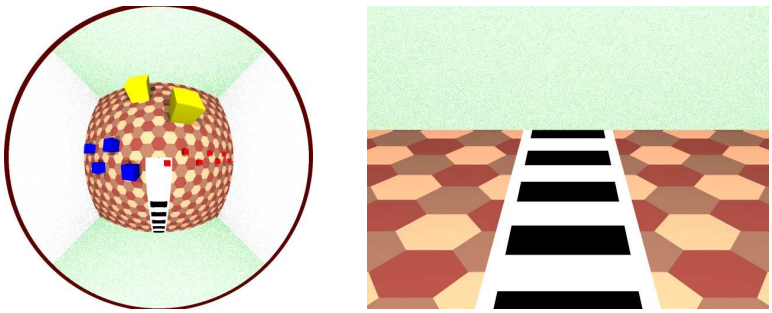

Fig. 3. Omnidirectional image (left) and traditional image (right) acquired by a virtual dual camera system in a synthetic room.

To better evaluate this result we also estimated the 3D position of the encircled corners belonging to the black squares visible in figure 4 (right): estimation results are reported in table 1 along with the ground truth values. Considering noise introduced by image quantization, that no interpolation methods were used to generate images, and that the omnidirectional has lower resolution than the traditional one, we can state that the spherical reprojection technique is suitable and effective also for Hybrid Dual Camera Vision System, as argued in the introduction.

4.2 Real Images

Tests on real images have been carried out exploiting the latest prototype of the HOPS (Hybrid Omnidirectional-Pinhole Sensor) sensor [3, 6, 15]. The effective-

[4] visit http://www.povray.org/ for more information

Workshop Proceedings of SIMPAR 2008
Intl. Conf. on SIMULATION, MODELING and PROGRAMMING for AUTONOMOUS ROBOTS
Venice(Italy) 2008 November,3-4
ISBN 978-88-95872-01-8
pp. 366-376

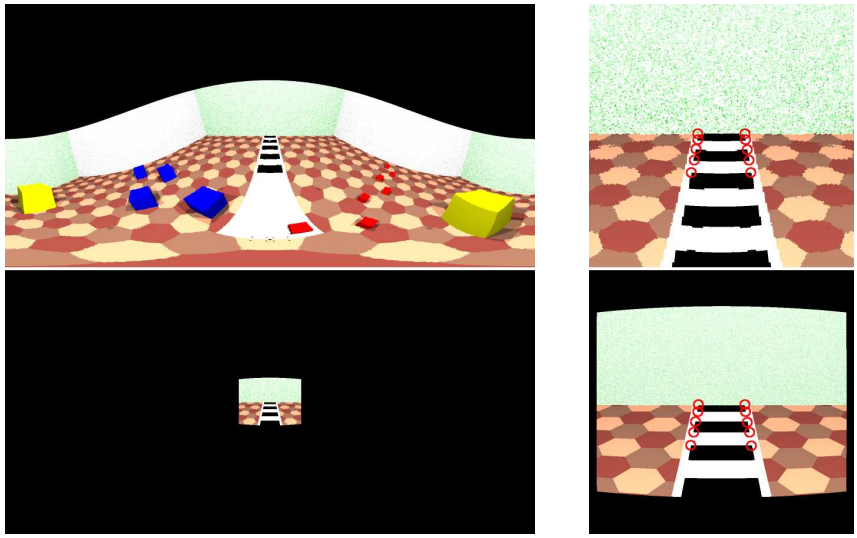

Fig. 4. Spherical rectification of the two images of figure 3: the upper image is derived from the omnidirectional one, while the lower one is derived from the traditional image. On the left, we show the whole sphere, while on the right we show a magnified detail referred to the common field of view of the two cameras: encircled corners are those used in the 3D position estimation test.

Table 1. 3D estimation results: estimated values (left side) compared with actual values (right side). The System reference frame was placed at (0.0, 0.0, 2000). All coordinates values are in mm.

Estimated Values			Real Values		
x	y	z	x	y	z
410.65	4009.62	-13.34	400.00	4000.00	0.00
-410.65	4009.61	-13.34	-400.00	4000.00	0.00
407.35	4407.41	-7.63	400.00	4400.00	0.00
-407.63	4409.53	-8.61	-400.00	4400.00	0.00
406.11	4795.37	-2.59	400.00	4800.00	0.00
-406.09	4795.13	-2.50	-400.00	4800.00	0.00
402.91	5182.88	7.64	400.00	5200.00	0.00
-402.81	5181.95	8.01	-400.00	5200.00	0.00
402.21	5462.87	13.70	400.00	5500.00	0.00
-401.43	5467.12	12.48	-400.00	5500.00	0.00

ness of this dual camera vision system derives from the joint use of a traditional camera and a central catadioptric camera which satisfies the single-viewpoint constraint: having two different viewpoints from which the world is observed, the sensor can therefore operate as a classical stereo pair.

Workshop Proceedings of SIMPAR 2008
Intl. Conf. on SIMULATION, MODELING and PROGRAMMING for AUTONOMOUS ROBOTS
Venice(Italy) 2008 November,3-4
ISBN 978-88-95872-01-8
pp. 366-376

Fig. 5. The latest version of the HOPS sensor.

Figure 5 shows the latest HOPS prototype. It uses two digital high-resolution Firewire cameras, in conjunction with mega-pixel lenses characterized by a very low TV-distortion, to achieve good image quality. The catadioptric part consists of a traditional camera pointing upwards to a hyperbolic mirror hanging over it and held by a plexiglas cylinder, while the traditional camera, hung to a stepper motor (controlled via a USB interface) and therefore able to rotate, has been placed in the lower part: this makes it possible to have no wires within the field of view of the omnidirectional image.

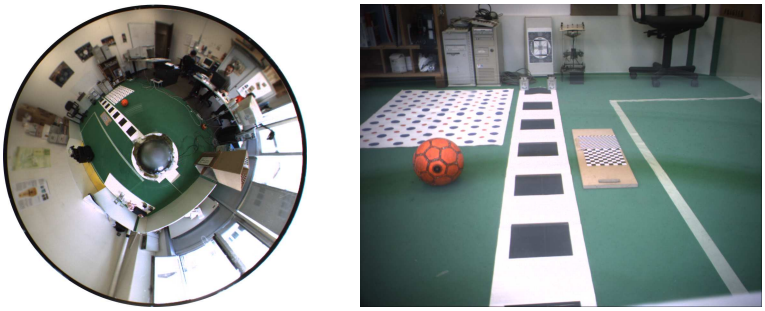

Fig. 6. Omnidirectional image (left) and traditional image (right) acquired by HOPS in an indoor room.

In figure 6 it is possible to see the two images acquired with HOPS and used in the test described in the sequel.

The calibration procedure developed for HOPS permits to evaluate all geometrical relationships subsisting between the two cameras. This means that, at any time, depending on the stepper position, it is possible to know the relative positioning of the reference frames of the two cameras and hence the exact position of the two viewpoints. In this way it is possible to apply the spherical reprojection procedure described above and thus obtain the rectified images shown in figure 7 (left).

Workshop Proceedings of SIMPAR 2008
Intl. Conf. on SIMULATION, MODELING and PROGRAMMING for AUTONOMOUS ROBOTS
Venice(Italy) 2008 November,3-4
ISBN 978-88-95872-01-8
pp. 366-376

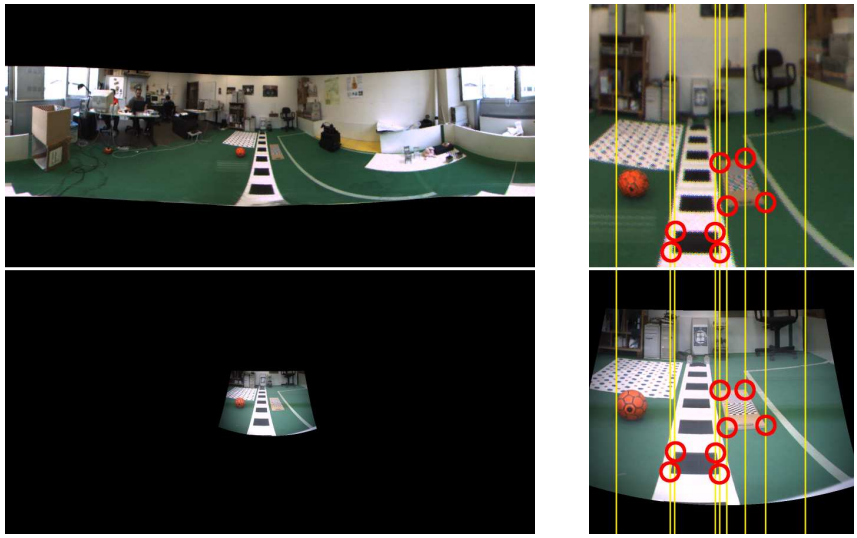

Fig. 7. Spherical rectification of the two images of figure 6: the upper image derives from the omnidirectional image, while the lower one derives from the traditional image. The whole sphere is shown on the left, while a magnified detail referred of the common field of view of the two cameras is shown on the right: the yellow lines highlight the correctness of epipolar line correspondence; encircled corners are those used in the 3D position estimation test.

Yellow lines in figure 7 (right), which shows a magnified detail of the common field of view of the two cameras, help verify the correct alignment of vertical epipolar lines. As can be observed, the resulting low resolution of the omnidirectional reprojection, along with the artifacts introduced by the de-bayering of the image, hamper precise location of features point. In any case, we estimated the 3D coordinates of the points highlighted in figure 7 (right) taking as their coordinates the output of a sub-pixel corner detector run on their surroundings.

The results obtained are shown in table 2. Since we do not know the ground truth values for the corners' positions, we can take the estimated sizes of the two objects as an evaluation criterion. The mean side length of the black square resulted 216 mm, with a standard deviation of 30 (its actual size is 200 mm), while the long sides of the wooden board resulted 725 mm and 676 mm and the short sides resulted 258 mm and 255 mm (the actual size of the board is 700×230 mm). Furthermore, the z coordinates of the points belonging to the black square should be all zero, while those belonging from the upper face of the wooden board should be all 16 mm (which is the board thickness). Finally, although obvious, the angle between each pair of adjacent sides should be ninety degrees. The error amounts to about 3% and confirms the results of previous experiments presented in [15].

Workshop Proceedings of SIMPAR 2008
Intl. Conf. on SIMULATION, MODELING and PROGRAMMING for AUTONOMOUS ROBOTS
Venice(Italy) 2008 November,3-4
ISBN 978-88-95872-01-8
pp. 366-376

Table 2. 3D estimation results: points' coordinates and lengths are in mm, while angles are expressed in degrees. The actual dimensions are 700×230 for the wooden board and 200×200 for the black square.

wooden board

corners	x	y	z	sides		angles	
1	1332.96	739.18	26.01		258.63		87.86
2	1143.82	915.58	24.70		676.98		103.03
3	1623.60	1393.01	38.18		254.99		77.70
4	1839.29	1258.28	19.46		725.17		91.28

black square

corners	x	y	z	sides		angles	
1	776.33	662.25	-3.22		246.28		93.05
2	617.98	850.80	-8.38		182.23		90.88
3	750.54	975.15	4.76		235.75		91.86
4	914.85	806.46	-6.47		199.99		83.85

The computation time required on a Intel® Core™2 Duo processor running at 3.80GHz to run rectification (that is far from being fully optimized) is about 0.6 seconds: considering the high resolution of the images involved in the process, it is a promising result. The possible use of look-up tables to re-project the images along with some other improvements to be applied to the code, could indeed permit to save processing time and obtain an application suitable for real-time spherical stereo processing.

5 Conclusions and Future Work

In this work we have showed how the spherical reprojection is particularly well suited for stereo vision with hybrid dual camera system. The geometrical framework to be employed has been carefully described and results obtained with both synthetic and real images have been showed confirming the effectiveness of the proposed approach.

As future work, we plan to investigate the employment of the rectified images obtained with this technique to build disparity/depth maps for hybrid sensors, and in particular for our HOPS prototype, placed on board of an autonomous/holonomous robot.

References

1. Nayar, S., Boult, T.: Omnidirectional vision systems: 1998 PI report (1997)
2. Cui, Y., Samarasekera, S., Huang, Q., Greiffenhagen, M.: Indoor Monitoring Via the Collaboration Between a Peripheral Sensor and a Fovea1 Sensor. In: VS '98: Proceedings of the 1998 IEEE Workshop on Visual Surveillance. Volume 00., Washington, DC, USA, IEEE Computer Society (1998) 2–9

Workshop Proceedings of SIMPAR 2008
Intl. Conf. on SIMULATION, MODELING and PROGRAMMING for AUTONOMOUS ROBOTS
Venice(Italy) 2008 November,3-4
ISBN 978-88-95872-01-8
pp. 366-376

3. Adorni, G., Cagnoni, S., Mordonini, M., Sgorbissa, A.: Omnidirectional stereo systems for robot navigation. In: Proceedings of the IEEE Workshop on Omnidirectional Vision (OMNIVIS 2003), Los Alamitos, IEEE Computer Society Press (2003)
4. Scotti, G., Marcenaro, L., Coelho, C., Selvaggi, F., Regazzoni, C.: Dual camera intelligent sensor for high definition 360 degrees surveillance. In: IEE Proceedings on Vision, Image and Signal Processing. Volume 152. (2005) 250–257
5. Yi Yao, Besma Abidi, Mongi Abidi: Fusion of Omnidirectional and PTZ Cameras for Accurate Cooperative Tracking. In: AVSS '06: Proceedings of the IEEE International Conference on Video and Signal Based Surveillance, Washington, DC, USA, IEEE Computer Society (2006) 46
6. Cagnoni, S., Mordonini, M., Mussi, L., Adorni, G.: Hybrid Stereo Sensor with Omnidirectional Vision Capabilities: Overview and Calibration Procedures. In: ICIAP 2007 - 14th International Conference on Image Analysis and Processing. (September 2007) 99–104
7. Cagnoni, S., Mordonini, M., Mussi, L., Adorni, G. Hybrid Dual Camera Vision Systems. In: Encyclopedia of Artificial Intelligence. IGI Global, Hershey, USA (May 2008) 848–852
8. Arican, Z., Frossard, P.: Dense Disparity Estimation from Omnidirectional Images. In: Proocedings of the 2007 IEEE International Conference on Advanced Video and Signal based Surveillance, IEEE Computer Society (September 2007) 399–404
9. Li, S.: Real-Time Spherical Stereo. In: 18th International Conference on Pattern Recognition, 2006. ICPR 2006. Volume 3. (0-0 2006) 1046–1049
10. Wan, D., Zhou, J., Zhang, D.: A Spherical Rectification for Dual-PTZ-Camera System. In: IEEE International Conference on Acoustics, Speech and Signal Processing, 2007. ICASSP 2007. Volume 1. (April 2007) I–777–I–780
11. Hicks, R.A., Perline, R.K.: Equiresolution catadioptric sensors. Applied Optics **44**(29) (October 2005) 6108–6114
12. Koji Yoshida, Hajime Nagahara, Masahiko Yachida: An Omnidirectional Vision Sensor with Single Viewpoint and Constant Resolution. In: International Conference on Intelligent Robots and Systems, 2006 IEEE/RSJ. (Oct. 2006) 4792–4797
13. Christopher Geyer, Kostas Daniilidis: Catadioptric Projective Geometry. International Journal of Computer Vision **45**(3) (2001) 223–243
14. Scaramuzza, D., Siegwart, R.: A New Method and Toolbox for Easily Calibrating Omnidirectional Cameras. In: 5th International Conference on Computer Vision Systems (ICVS). (March 2007)
15. Cagnoni, S., Mordonini, M., Mussi, L., Adorni, G. HOPS - A Hybrid Dual Camera Vision System. In: Encyclopedia of Artificial Intelligence. IGI Global, Hershey, USA (May 2008) 840–847

Workshop Proceedings of SIMPAR 2008
Intl. Conf. on SIMULATION, MODELING and PROGRAMMING for AUTONOMOUS ROBOTS
Venice(Italy) 2008 November,3-4
ISBN 978-88-95872-01-8
pp. 366-376